

Mode- and Direction-Dependent Mechanical Energy Dissipation in Single-Crystal Resonators due to Anharmonic Phonon-Phonon Scattering

Srikanth S. Iyer*

Department of Electrical Engineering, University of California, Los Angeles, California 90095, USA

Robert N. Candler

*Department of Electrical Engineering, University of California, Los Angeles, California 90095, USA
and California NanoSystems Institute, Los Angeles, California 90095, USA*

(Received 1 October 2015; revised manuscript received 16 December 2015; published 4 March 2016)

In this work, we determine the intrinsic mechanical energy dissipation limit for single-crystal resonators due to anharmonic phonon-phonon scattering in the Akhiezer ($\Omega\tau \ll 1$) regime. The energy loss is derived using perturbation theory and the linearized Boltzmann transport equation for phonons, and includes the direction- and polarization-dependent mode-Grüneisen parameters in order to capture the strain-induced anharmonicity among phonon branches. This expression reveals the fundamental differences among the internal friction limits for different types of bulk-mode elastic waves. For cubic crystals, 2D-extensional modes have increased dissipation compared to width-extensional modes because the biaxial deformation opposes the natural Poisson contraction of the solid. Additionally, we show that shear-mode vibrations, which preserve volume, have significantly reduced energy loss because dissipative phonon-phonon scattering is restricted to pure-shear phonon branches, indicating that Lamé- or wineglass-mode resonators will have the highest upper limit on mechanical efficiency. Finally, we employ key simplifications to evaluate the quality factor limits for common mode shapes in single-crystal silicon devices, explicitly including the correct effective elastic storage moduli for different vibration modes and crystal orientations. Our expression satisfies the pressing need for a reliable analytical model that can predict the phonon-phonon dissipation limits for modern resonant microelectromechanical systems, where precise manufacturing techniques and accurate finite-element methods can be used to select particular vibrational mode shapes and crystal orientations.

DOI: [10.1103/PhysRevApplied.5.034002](https://doi.org/10.1103/PhysRevApplied.5.034002)

I. INTRODUCTION

The performance of mechanical resonators is governed by the dissipation of energy stored in the resonant vibrational mode to other acoustic modes or the environment [1]. Despite the increasing prevalence of resonant microelectromechanical systems as high-performance inertial sensors, mass-based chemical sensors, timing references, and frequency filters, the energy dissipation in these structures is not well understood [2]. The dissipation can be difficult to determine because there is no single, predictive theory to evaluate the quality factor (Q), defined as $2\pi[(\text{energy stored})/(\text{energy loss per cycle})]$. A number of damping mechanisms, each requiring its own unique physical model, may contribute to the dissipation; however, the losses add linearly, so the quality factors add reciprocally and a single loss mechanism will dominate for a particular set of operating conditions [3]. The accurate prediction of Q has tremendous design implications because it is directly related to device performance metrics including sensitivity for resonant sensors, bandwidth for radio-frequency filters, and phase noise for timing references.

Energy-loss mechanisms may be intrinsic, fundamental to the material and device geometry, or extrinsic, a function of the operating environment of the resonator. This work focuses on determining intrinsic dissipation limits in dielectric and semiconductor crystals, which are governed by the interaction between the elastic wave and thermal phonons. This interaction, also called internal friction, has two components: spatial phonon transport and local phonon scattering. Time-varying strain gradients drive irreversible spatial phonon transport (heat flow), known as thermoelastic dissipation (TED). TED is a well-understood loss mechanism that can be accurately predicted using a finite-element solver and can be minimized via the appropriate design of device geometry [4,5]. Moreover, it is negligible for vibration modes with uniform strain, because there are no strain-induced thermal gradients, and it becomes less significant as resonators approach the GHz regime due to a mismatch between the time constant for heat transfer and the mechanical vibration period. Thus, for high-frequency and bulk-mode resonators, the dissipation is ultimately limited by local phonon-phonon scattering, commonly referred to as Akhiezer damping. In this work, we derive an expression for Akhiezer loss that captures the effect of anharmonic phonon-phonon scattering as well as crystalline anisotropy.

*ssiyer@ucla.edu

In the Akhiezer damping model, the strain produced by the mechanical wave modulates the phonon frequencies and, consequently, the local equilibrium phonon distribution. The phonon populations cannot change instantaneously and will relax towards the modulated equilibrium distribution via phonon-phonon scattering when the thermal relaxation time (τ) is significantly less than the period of the mechanical wave. Because of the application of rapidly varying strain and a finite τ , the time-dependent phonon populations lag behind their (perturbed) equilibrium value. This relaxation towards equilibrium is an entropy-producing process that consumes energy from the elastic wave. It is important to note that the Akhiezer damping model applies only when the scattering rate ($1/\tau$) is significantly larger than the frequency (Ω) of the mechanical vibration $\Omega\tau \ll 1$, which is the case at room temperature for commonly used acoustic materials such as silicon, germanium, and quartz [6].

This limit on mechanical energy dissipation was first described by Akhiezer [7] and later solved by Woodruff using the linearized Boltzmann transport equation (BTE) and the Debye approximation to arrive at a simplified expression for internal friction (Q^{-1}) involving only classical, bulk parameters [8].

$$Q^{-1} = \frac{\gamma_0^2 C_v T}{\rho c^2} \Omega \tau. \quad (1)$$

In the above expression, T is the ambient temperature, ρ is the material density, c is the Debye average sound velocity, C_v is the specific heat per unit volume, and γ_0 is the average Grüneisen parameter associated with thermal expansion. Woodruff derives this result by assuming that all phonon modes are perturbed identically by the strain wave and neglecting the perturbation of the internal temperature of the solid. Typically, this expression is used to make an order of magnitude prediction of the internal friction limit in a given material [9].

Mason provides an alternate approach, arriving at an expression for internal friction by taking the derivative of the total phonon energy with respect to the applied strain and interpreting this as a loss modulus in accordance with Zener's phenomenological theory of anelastic relaxation in solids [10,11]. Critically, Mason shows that because the dissipation originates from anharmonicity of phonon modes, third-order elastic coefficients can be used to estimate the mode-Grüneisen parameters γ_i , which represent the strength of the phonon frequency perturbation to an applied strain for a particular pure phonon mode i , characterized by a crystal direction and polarization. Thus, Mason dispenses with the assumption that all phonon branches have the same γ_i in an attempt to provide a more accurate estimate of the Akhiezer damping limit.

Mason's derivation was heavily criticized by Barrett and Holland because of its lack of analytical rigor [12]; the most

notable objections were the seemingly arbitrary designation of certain phonon frequency terms as strain independent and the cursory assumption that the cutoff frequency in the Debye integral is strain independent. Nevertheless, Mason's expression for acoustic attenuation appeared to provide better agreement with experimental results in silicon and germanium than Woodruff's simpler but more analytically sound expression. Consequently, Mason's (incorrect) expression is often cited when attempting to fit experimental data while Woodruff's is used to provide an upper bound on Q for a given material system [9,13]. A few refinements to Mason's method have been introduced, including a correction factor for the Debye integral to account for the modulation of the upper integration limit [14] and Brugger-Fritz integration schemes to include phonon scattering to arbitrary directions [15]. Even with these corrections, Mason's expression is inherently flawed [16], so it should not be used to predict experimental results. Similarly, in an attempt to better match acoustic attenuation measurements, Nava *et al.* modified Woodruff's method by introducing a pure-mode ultrasonic Grüneisen parameter. They rigorously define this parameter as a weighted average of mode-specific phonon thermal conductivities, but cannot evaluate their complex expression and instead simply fit its value to experimental results [17]. Ultimately, all of these refinements require careful integration over the spectrum of acoustic phonon modes, which unnecessarily complicates the evaluation of the energy dissipation.

More recently, Kiselev and Iafrate considered the internal friction for the specific case of a doubly-clamped, flexural-mode cantilever and, following the approach introduced by Bömmel and Dransfeld, showed qualitatively that the anharmonicity induced by the presence of just two groups of phonons with different mode-Grüneisen parameters results in local phonon-phonon dissipation [18,19]. However, they oversimplify their evaluation of the dissipation limit by assuming only two phonon groups and arbitrarily designating values for the mode-Grüneisen parameters for each group, prohibiting a valid comparison with experimental data. Kunal and Aluru used molecular dynamics to calculate the Akhiezer limit for nickel nanowires with a maximum size of 20 atoms per edge [20]. Ultimately, likely due to the resonator size restriction imposed by the practical computational limitations, they do not compare the molecular dynamics results to experimental data, and only attempt to correlate their results to existing theory by evaluating Mason's nonlinearity parameter D , which we have already indicated is not an analytically sound choice. Hence, there is a compelling need for a more predictive, analytical model that employs appropriate simplifications so that the energy loss can be evaluated in a straightforward and consistent manner using known material constants and reliably compared with experimental results.

In this work, we rigorously derive an expression for the internal friction limit due to anharmonic phonon-phonon scattering that incorporates important elements of both Woodruff's and Mason's derivations. We solve for the energy loss using the analytically sound Boltzmann transport method, but rather than assuming all phonon modes are perturbed equally by strain, we include the directional- and polarization-dependent mode-Grüneisen parameters. The resulting expression for Akhiezer damping still depends only on bulk parameters, but distinguishes between different vibration modes and crystal directions. As we will show, for common vibration modes this expression can be reduced to match Eq. (1), but replacing the average Grüneisen parameter γ_0 with an anharmonic Grüneisen parameter Γ_a that depends on the strain profile of the vibration.

II. ENERGY LOSS

The derivation of the anharmonic phonon-phonon dissipation begins with the assumption that the strain wave is time harmonic with wave vector \mathbf{K} and angular frequency Ω so that $\epsilon(t) \propto \exp[i(\mathbf{K} \cdot \mathbf{r} - \Omega t)]$, where \mathbf{r} is the position vector. The strain perturbs the frequencies (ω) of all thermal phonons, satisfying the relation

$$\omega_i = \omega_{i0}[1 + \vec{\gamma}_i \cdot \vec{\epsilon}(t)] = \omega_{i0} + \Delta\omega_i, \quad (2)$$

where the index i denotes a pure-mode branch characterized by a direction and polarization along a crystal axis so that ω_i is the instantaneous phonon frequency of the i th branch and ω_{i0} is the unperturbed equilibrium phonon frequency. Each high-symmetry direction in the Wigner-Seitz cell, the primitive Brillouin zone, has a longitudinal mode that is polarized along the direction of phonon propagation and two transverse modes that are polarized perpendicularly to the propagation direction. Figure 1 shows the 13 principal crystallographic directions (high-symmetry directions) in the Wigner-Seitz cell for the diamond lattice with the $\langle 100 \rangle$, $\langle 110 \rangle$, and $\langle 111 \rangle$ families of directions in distinct subplots. Deformation of the solid due to strain, even in just a single direction, deforms the entire Brillouin zone, resulting in the perturbation of all phonon branches.

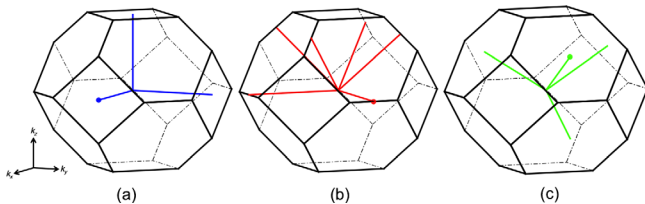


FIG. 1. Wigner-Seitz cell for the diamond lattice centered about the Γ point. (a) Three $\langle 100 \rangle$ directions (blue). (b) Six $\langle 110 \rangle$ directions (red). (c) Four $\langle 111 \rangle$ directions (green). There are 13 high-symmetry crystal directions and each contributes three pure modes, one longitudinal and two transverse, resulting in 39 distinct phonon branches.

For cubic crystals, the strain tensor is assumed to be symmetric, so we can express it compactly as a vector $\vec{\epsilon}(t)$, with six independent components, denoted ϵ_j , where the index j indicates one of the six possible strain directions: three normal and three shear [see Eq. (3)].

$$\begin{bmatrix} \epsilon_{xx} \\ \epsilon_{yy} \\ \epsilon_{zz} \\ \epsilon_{yz} \\ \epsilon_{zx} \\ \epsilon_{xy} \end{bmatrix} = \begin{bmatrix} \epsilon_1 \\ \epsilon_2 \\ \epsilon_3 \\ \epsilon_4 \\ \epsilon_5 \\ \epsilon_6 \end{bmatrix}. \quad (3)$$

Consequently, $\vec{\gamma}_i$ is also a vector with six components that are the mode-Grüneisen parameters $\gamma_{i,j}$, corresponding to the anharmonic perturbation of the i th branch frequency due to strain in the j th direction. Here, we assume that the $\gamma_{i,j}$'s are independent of the phonon frequency and wave number. As a result, the instantaneous phonon population in each branch N_i deviates from its thermal equilibrium Bose-Einstein distribution $N_{i0} = (e^{\hbar\omega_{i0}/k_B T} - 1)^{-1}$ so that

$$N_i = N_{i0} + \Delta n_i. \quad (4)$$

Now, we use the linearized BTE to solve for N_i . We derive the dissipation limit due to local phonon-phonon scattering, so we assume uniform strain and can eliminate all spatial terms in the BTE. Thus, the relaxation towards equilibrium is solely determined by the scattering term

$$\left. \frac{\partial N_i}{\partial t} \right|_{\text{scatt}} = \frac{\partial N_i}{\partial t}. \quad (5)$$

Following the approach of Woodruff and others [12,17], we employ the relaxation time approximation to describe the scattering term as the decay of N_i towards a Bose-Einstein distribution N'_{i0} at a modulated local temperature $T' = T + \Delta T$.

$$\frac{\partial N_i}{\partial t} = \frac{N_i - N'_{i0}}{\tau}, \quad (6)$$

where

$$N'_{i0} = (e^{\hbar\omega_i/k_B T'} - 1)^{-1} \quad (7)$$

and τ is the average time between phonon collisions. The mode-specific time constants τ_i are not all available, so we make the practical assumption that τ is the same for all acoustic modes. Figure 2 outlines the perturbation theory and the corresponding dissipative relaxation.

Solving BTE assuming plane wave solutions, $\Delta\omega_i$, Δn_i , $\Delta T \propto \exp[i(\mathbf{K} \cdot \mathbf{r} - \Omega t)]$, yields

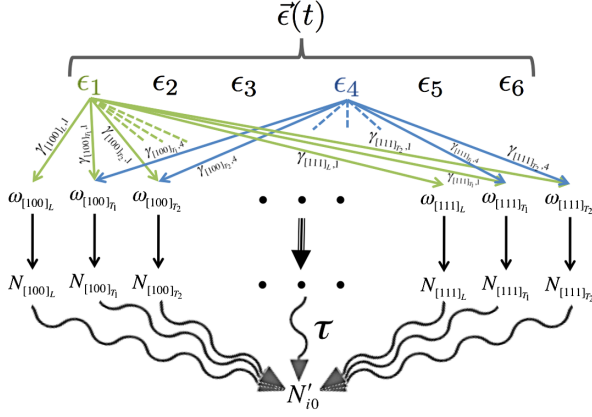


FIG. 2. Overview of the energy loss due to anharmonic phonon-phonon scattering. Strain in one of the normal directions ϵ_{1-3} leads to a perturbation of phonon frequencies in each branch, characterized by the mode-Grüneisen parameter $\gamma_{i,j}$, where j is the strain direction and i represents the crystal direction and polarization. For the diamond lattice, we can express i using the notation $[hkl]_P$, where $[hkl]$ is a particular crystal direction (expressed using Miller indices) and P is the polarization, which can be either longitudinal (L) or transverse (T_1 or T_2). The modulation of phonon frequencies (and energies) means the respective branch populations are out of equilibrium. Each branch distribution relaxes towards the perturbed equilibrium distribution via phonon-phonon scattering. The energy loss that occurs during this irreversible relaxation process is assumed to come from the acoustic wave, because that is the source of the perturbation. The shear strains ϵ_{4-6} , however, only perturb the phonon frequencies in branches with transverse polarizations, because a volume change is prohibited. Hence, shear-mode vibrations tend to have reduced dissipation because only a fraction of the phonon branches contribute to the loss.

$$\Delta n_i = \omega_{i0} \left(\frac{\partial N'_{i0}}{\partial \omega_i} \right)_0 \left(\frac{\Delta \omega_i}{\omega_{i0}} - \frac{\Delta T}{T} \right) (1 - i\Omega\tau)^{-1}. \quad (8)$$

After evaluating the partial derivative and combining terms, we have

$$\Delta n_i = \left(-\frac{TC_{k,i}}{\hbar\omega_{i0}} \right) \left(\frac{\Delta \omega_i}{\omega_{i0}} - \frac{\Delta T}{T} \right) (1 - i\Omega\tau)^{-1}, \quad (9)$$

where $C_{k,i}$ is the specific heat contribution from a particular phonon mode that depends on the branch i and the phonon wave vector k . It can be written explicitly as

$$C_{k,i} = \frac{(\hbar\omega_{i0})^2 e^{\hbar\omega_i/k_B T}}{k_B T^2 (e^{\hbar\omega_{i0}/k_B T} - 1)^2} \quad (10)$$

and is related to the classical specific heat per unit volume using

$$C_v = \sum_{k,i} C_{k,i}, \quad (11)$$

where the subscripts indicate a summation over all acoustic phonon modes, specified by k and i .

For clarity, we proceed with the remainder of the derivation assuming uniaxial strain [i.e., $\vec{\epsilon}(t) = \epsilon_j$]. We will show later how to make the appropriate modifications to capture the effect in realistically achievable vibration modes where Poisson contraction leads to the deformation of more than one strain component. Under this uniaxial assumption, Eq. (2) reduces to

$$\frac{\Delta \omega_i}{\omega_{i0}} = \gamma_{i,j} \epsilon(t) \quad (12)$$

because ϵ_j is the only nonzero strain component so that only the j th component of $\vec{\gamma}_i$ (indicated by the second subscript) contributes to the anharmonicity. As shown by Akhiezer, the temperature modulation can be determined self-consistently using the condition that the collision process conserve energy to first order [7,12], giving

$$\frac{\Delta T}{T} = \sum_{k,i} C_{k,i} \frac{\Delta \omega_i}{\omega_{i0}} (1 - i\Omega\tau)^{-1} / \sum_{k,i} C_{k,i} (1 - i\Omega\tau)^{-1}. \quad (13)$$

We can express this succinctly as

$$\frac{\Delta T}{T} = \langle \gamma_{i,j} \rangle \epsilon(t), \quad (14)$$

where $\langle \gamma_{i,j} \rangle$ is the average of the j th component of each $\vec{\gamma}_i$, weighted by its contribution to the total specific heat, over all phonon branches. Substituting Eqs. (12) and (14) into the solution to the BTE gives

$$\Delta n_i = \left(-\frac{TC_{k,i}}{\hbar\omega_{i0}} \right) (\gamma_{i,j} - \langle \gamma_{i,j} \rangle) \epsilon(t) (1 - i\Omega\tau)^{-1}. \quad (15)$$

Now, we can proceed with the energy loss calculation. The energy loss per cycle of oscillation is simply the time average of the rate at which energy is lost via phonon-phonon scattering,

$$U_{\text{loss per cycle}} = - \sum_{k,i} \left\langle H_i \left(\frac{\partial N_i}{\partial t} \right)_{\text{scatt}} \right\rangle_{\text{cycle}}, \quad (16)$$

where the $H_i = \hbar\omega_i$, is the phonon Hamiltonian and $\langle \cdot \rangle_{\text{cycle}}$ denotes the time average over one period of the mechanical vibration $2\pi/\Omega$. We can rewrite this using the chain rule for derivatives,

$$U_{\text{loss per cycle}} = - \sum_{k,i} \left\langle N_i \frac{\partial H_i}{\partial t} - \frac{\partial (N_i H_i)}{\partial t} \right\rangle_{\text{cycle}}. \quad (17)$$

The second term is simply the time derivative of the total energy, which we can eliminate because it must be constant

in time. Because of the time average over one cycle, only the time-harmonic component of N_i contributes to the loss, so we can ignore N_{i0} and

$$U_{\text{loss per cycle}} = -\sum_{k,i} \left\langle \Delta n_i \frac{\partial H_i}{\partial t} \right\rangle_{\text{cycle}}. \quad (18)$$

Substituting the solution to the BTE in Eq. (15) and evaluating the derivative yields

$$U_{\text{loss per cycle}} = -\sum_{k,i} TC_{k,i} \frac{\gamma_i(\gamma_i - \langle \gamma_{i,j} \rangle)}{1 - i\Omega\tau} i\Omega \langle \epsilon^2(t) \rangle_{\text{cycle}} \quad (19)$$

after removing the time-independent terms from the $\langle \cdot \rangle_{\text{cycle}}$ brackets. Noticing that $\langle \epsilon^2(t) \rangle_{\text{cycle}} = (\pi/\Omega)\epsilon_0^2$, where ϵ_0 is the amplitude of the strain wave, and taking the real part of the energy loss reduces this to

$$U_{\text{loss per cycle}} = \sum_{k,i} TC_{k,i} (\gamma_{i,j}^2 - \langle \gamma_{i,j} \rangle^2) \pi \epsilon_0^2 \frac{\Omega\tau}{1 + \Omega^2\tau^2}. \quad (20)$$

Assuming each branch contributes equally to the total phonon specific heat, we can eliminate the cumbersome summation and express the energy loss as

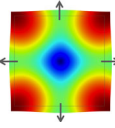
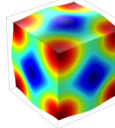
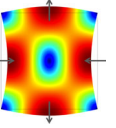
$$U_{\text{loss per cycle}} = \pi (\langle \gamma_{i,j}^2 \rangle - \langle \gamma_{i,j} \rangle^2) C_v T \epsilon_0^2 \frac{\Omega\tau}{1 + \Omega^2\tau^2}, \quad (21)$$

where the angle brackets indicate an average over all phonon branches. If the second- and third-order elastic coefficients are known, theoretical values for $\gamma_{i,j}$ can be obtained [6] and the energy-loss expression can be calculated using only bulk parameters. Ultimately, as we will show in Sec. V, the total energy loss can be expressed as the superposition of the uniaxial losses. The remaining sections show how to normalize the loss for the strain magnitude so we can evaluate the loss and compare the performance of different devices in a given material system.

III. ENERGY STORAGE

The quality factor is a ratio of energy stored to energy lost per cycle, so it is important to account for the anisotropy and mode dependence in both. For cubic crystals, the energy storage is anisotropic and depends on the deformation profile. The elasticity of the crystal can be described by relating stress ($\vec{\sigma}$) and strain ($\vec{\epsilon}$) using the second-order elastic tensor.

TABLE I. Displacement profiles and elastic storage moduli for common vibration modes of a single-crystal rectangular parallelepiped with edges oriented along the [100] directions.

| Width extensional | Square extensional | Cubic extensional | Lamé (shear) |
|---|---|---|---|
|  |  |  |  |
| $\frac{(c_{11}-c_{12})(c_{11}+2c_{12})}{c_{11}+c_{12}}$ | $c_{11} + c_{12} - \frac{2c_{12}^2}{c_{11}}$ | $\frac{c_{11}+2c_{12}}{3}$ | c_{44} |

$$\vec{\sigma} = \begin{bmatrix} c_{11} & c_{12} & c_{12} & 0 & 0 & 0 \\ c_{12} & c_{11} & c_{12} & 0 & 0 & 0 \\ c_{12} & c_{12} & c_{11} & 0 & 0 & 0 \\ 0 & 0 & 0 & c_{44} & 0 & 0 \\ 0 & 0 & 0 & 0 & c_{44} & 0 \\ 0 & 0 & 0 & 0 & 0 & c_{44} \end{bmatrix} \cdot \vec{\epsilon}. \quad (22)$$

Here, appropriate simplifications are made given cubic symmetry and the equivalence of shear directions, so that the elasticity matrix can be described using only three components c_{11} , c_{12} , and c_{44} .

For a given vibration mode and orientation, an effective Young's modulus or storage modulus E_{eff} can be defined so that the energy storage per unit volume is $E_{\text{stored}} = \frac{1}{2} E_{\text{eff}} \epsilon_0^2$ [21]. For spatially uniform modes, we can eliminate the integral over the volume of the structure, because the energy storage (and loss) in any volume element of the solid is the same. The modes of interest are width extensional (WE), square extensional (SE), cubic extensional (CE), and Lamé; their deformation profiles and expressions for effective storage moduli are given in Table I. These are commonly used vibration modes for a single-crystal rectangular parallelepiped with edges oriented along the [100] axes. The WE, SE, and CE modes are modes where the deformation of the solid is primarily due to extension (and contraction) along one, two, or three principal axes, respectively. The Lamé mode (also called a "contour" mode) is a pure-shear mode with only one nonzero strain component.

IV. QUALITY FACTOR

Using the definition of the quality factor, the energy storage expression in the previous section, and the energy loss in Eq. (21), we can write the quality factor as

$$Q = \frac{E_{\text{eff}}}{(\langle \gamma_{i,j}^2 \rangle - \langle \gamma_{i,j} \rangle^2) C_v T} \frac{1 + \Omega^2\tau^2}{\Omega\tau} \quad (23)$$

for the uniaxial case. If we employ Woodruff's simplifications that the material is isotropic so all $\gamma_{i,j} = \gamma_0$ and that $\Delta T = 0$, and assume the storage modulus is simply the bulk modulus $B = \rho c^2$, this expression reduces identically to Eq. (1) in the low-frequency limit. This result is expected because both methods use the BTE to determine the energy loss. Woodruff's assumptions allow for simple estimation of Q using bulk material data, but it is important to note that these assumptions are not self-consistent. If the material is assumed to be isotropic and all $\gamma_{i,j} = \gamma_0$, then the average $\langle \gamma_{i,j} \rangle = \gamma_0$ which implies that $\Delta T \neq 0$. In fact, when this assumption is employed rigorously, $\langle \gamma_{i,j}^2 \rangle = \langle \gamma_{i,j} \rangle^2 = \gamma_0^2$ and the dissipation in Eq. (21) is zero. We also note that the result derived here does in fact match Zener's expression for quality factor due to anelastic relaxations in a solid. This suggests that Mason's method can also be used to obtain the same result, although we do not include it here [22]. Briefly, Mason's simplification is approximately valid in the low-temperature limit, where the upper integration limit in the Debye integral approaches infinity and the assumption that the integration limits are strain independent is satisfied. In this low-temperature limit, the total acoustic phonon energy $U_0 \approx C_v T/4$. This is precisely the condition that reveals the T^3 dependence of the low-temperature Debye specific heat in insulators [23]. This likely explains the persistent deviation from experimental values at high temperatures when employing modified versions of Mason's expression for acoustic attenuation [13]. Even if these low-temperature conditions are satisfied, Mason's expression omits a factor of 4, which is produced when proper care is taken to include the strain dependence of all phonon frequency terms [12].

V. MODE-DEPENDENT ENERGY LOSS

The expression in Eq. (23) accounts for the anisotropic and mode-dependent energy storage, but still only includes loss due to strain in a single direction. In order to more accurately determine the losses, we define an effective mode-Grüneisen parameter $\gamma_{i,\text{eff}}$ as the weighted average of the components of $\vec{\gamma}_i$ by their corresponding strain component ϵ_j . Thus, we can capture the perturbation of the phonon branch frequency due to strain in more than one direction.

For cubic crystals, symmetry dictates that $\langle \gamma_{i,1} \rangle = \langle \gamma_{i,2} \rangle = \langle \gamma_{i,3} \rangle$ and the equivalence of shear directions implies $\langle \gamma_{i,4} \rangle = \langle \gamma_{i,5} \rangle = \langle \gamma_{i,6} \rangle$. For pure extensional vibration modes the shear strain components are all zero. Thus, the effective mode-Grüneisen parameter can be reduced to $\gamma_{i,\text{eff}} = \alpha \gamma_{i,1}$, where α is a coefficient determined by the relative axial strain in the x , y , and z directions. α is determined from the strain profile, so it is the same for all branches and the quality factor is simply reduced by a factor of $1/\alpha^2$. In order to retain the simplicity of Eq. (1), we express the quality factor as

$$Q = \frac{E_{\text{eff}}}{\Gamma_a^2 C_v T} \frac{1 + \Omega^2 \tau^2}{\Omega \tau} \quad (24)$$

and define the anharmonic Grüneisen parameter as

$$\Gamma_a^2 = \alpha^2 (\langle \gamma_{i,1}^2 \rangle - \langle \gamma_{i,1} \rangle^2). \quad (25)$$

Unlike Nava's pure-mode ultrasonic Grüneisen parameter, which can only be evaluated assuming a pure sound mode oriented and polarized along crystal axes, our anharmonic Grüneisen parameter accounts for the deformation in real mechanical modes, which are superpositions of pure modes and are determined from both material properties and the geometry of the structure. For pure-shear modes, which include Lamé modes, we can write $\gamma_{i,\text{eff}} = \alpha \gamma_{i,5}$ so that $\Gamma_a^2 = \alpha^2 (\langle \gamma_{i,5}^2 \rangle - \langle \gamma_{i,5} \rangle^2)$. Expressions for α^2 for vibration modes in cubic crystals are given in the first row of Table II. For vibrations that are a mix of both longitudinal and shear perturbations, γ_{eff} will be a weighted sum of $\gamma_{i,1}$ and $\gamma_{i,5}$ determined by the dot product in Eq. (2).

Equation (24) shows that the quality factor depends distinctly on the resonant frequency, due to a mismatch between the period of the elastic wave ($2\pi/\Omega$) and the phonon lifetime (τ), and the strain profile, due to fundamental differences in the strength of the phonon perturbation, which we quantify using α^2 . The resonant frequency and vibrational mode shape are, of course, fundamentally linked and should be solved simultaneously using the material properties and boundary conditions of the resonator in the mechanical eigenvalue problem.

Mason and Bateman establish that the mode-Grüneisen parameters can be determined from second- and third-order elastic moduli and calculate $\gamma_{i,1}$ and $\gamma_{i,5}$ for silicon and germanium [10]. Critically, they show that $\langle \gamma_{i,1} \rangle \approx \gamma_0$ as expected, because both averages relate to volume perturbation of the solid. They also verify that $\langle \gamma_{i,5} \rangle = 0$, which satisfies the restriction that shear deformations do not perturb volume. The simplified expressions for Γ_a^2 are included in the second row of Table II. Finally, equipped with the knowledge of $\gamma_{i,1}$ and $\gamma_{i,5}$, we can calculate $\langle \gamma_{i,1}^2 \rangle$ and $\langle \gamma_{i,5}^2 \rangle$ and evaluate Γ_a^2 .

TABLE II. Expressions for the strain deformation coefficient α^2 (row 1) and the anharmonic Grüneisen parameter Γ_a^2 (row 2) for the common vibration modes identified in Table I.

| | Width extensional | Square extensional | Cubic extensional | Lamé (shear) |
|--------------|--|--|--|---|
| α^2 | $\frac{(c_{11}-c_{12})^2}{c_{11}^2+2c_{11}c_{12}+3c_{12}^2}$ | $\frac{2(c_{11}-c_{12})^2}{c_{11}^2+2c_{12}^2}$ | 3 | 1 |
| Γ_a^2 | $\alpha^2 (\langle \gamma_{i,1}^2 \rangle - \gamma_0^2)$ | $\alpha^2 (\langle \gamma_{i,1}^2 \rangle - \gamma_0^2)$ | $\alpha^2 (\langle \gamma_{i,1}^2 \rangle - \gamma_0^2)$ | $\alpha^2 \langle \gamma_{i,5}^2 \rangle$ |

VI. RESULTS AND DISCUSSION

In this section, we evaluate the quality factor limits in silicon and compare the performance for common vibration modes. The final parameter needed to evaluate Q is the phonon lifetime τ . Following Woodruff's approach, we determine τ using the definition of bulk thermal conductivity $\kappa \equiv \frac{1}{3} C_v c^2 \tau$. This is, in effect, an average time constant over all phonon branches. Others have replaced the average phonon time constant τ with the direction-specific lifetimes $\tau_{[hkl]}$ corresponding to the particular crystal orientation of the mechanical vibration [24,25], but we assert that this is not the most accurate approach, because the strain perturbs phonon branches in *all* crystal directions, not just along the direction of sound propagation, making a collective relaxation time a better estimate. The most accurate approach would be to use the branch-specific τ_i , which depend on both direction and polarization; however, the lack of a complete set of experimental values for these time constants prohibits calculation in this way.

Figure 3 shows the room temperature $f \times Q$ product as a function of the mechanical resonant frequency for the WE, SE, CE, and Lamé modes of a resonator with edges oriented along the [100] directions in intrinsic silicon evaluated using the expression in Eq. (24) along with Woodruff's result for reference and a number of experimental results from silicon resonators in the literature [26–39]. As expected, given the quadratic dependence of Q on resonant frequency in the Zener model, the curves remain constant up to ~ 20.5 GHz, corresponding to the condition $\Omega\tau = 1$. Again, we note that the Akhiezer

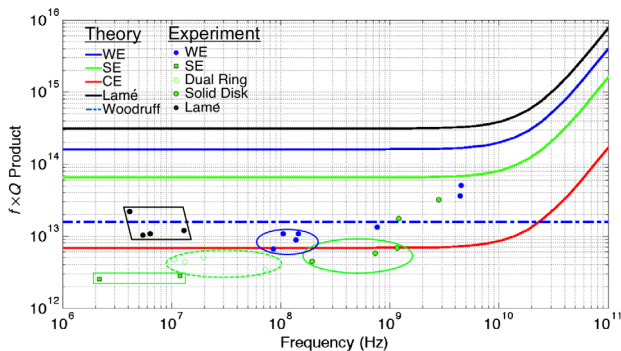


FIG. 3. Anharmonic and anisotropic $f \times Q$ product limits versus mechanical resonant frequency at room temperature for WE, SE, CE, and Lamé modes in [100] silicon. The solid lines represent the quality factor limits derived in this work [Eq. (24)]. The dashed line is Woodruff's estimation of the Akhiezer damping limit and the points are experimental results from high quality factor resonators surveyed from the literature [26–39]. A number of recently fabricated resonators have quality factors that exceed Woodruff's limit, indicating that the simplified, isotropic expression does not provide sufficient accuracy. The ungrouped points are measurements of higher-order harmonics, so the assumption in this work of uniform strain is not directly applicable.

damping model applies only when $\Omega \ll 1/\tau$, so the results should only be interpreted below this value; at higher frequencies, the strain varies faster than the phonon scattering rate, so the number of average collisions per cycle is severely reduced and an alternate model, often called Landau-Rumer dissipation, should be used instead [40]. We can equivalently express this condition as $l_{\text{ph}} \ll \lambda_{\text{ac}}$, where l_{ph} is the mean-free path for thermal phonons and λ_{ac} is the wavelength of the elastic wave. As a result, we can reframe the frequency cutoff as a minimum size limitation. A simple calculation (ignoring phonon dispersion) gives $l_{\text{ph}} \approx 47$ nm for silicon at room temperature. This means our damping model provides a valid picture of the phonon-phonon dynamics for resonators where all dimensions are greater than ~ 47 nm, which serves as a theoretical minimum cutoff size for bulk phonon phenomena in single-crystal silicon at room temperature. We note, however, that Ju and Goodson report average phonon mean-free paths of ~ 300 nm in thin silicon layers via thermal conductivity measurements [41] and more recent work provides evidence of a broad spectrum of phonon mean-free paths in silicon, where phonons with $l_{\text{ph}} > 1 \mu\text{m}$ contribute significantly to the thermal conductivity [42,43].

The (solid) theory curves show that the upper limit on Q for the WE mode is greater than that of the SE mode, which is, in turn, larger than the CE mode. This result can be inferred from the deformation constants α^2 derived in Sec. V. In the WE mode, the structure expands in the x direction and contracts in both the y and z directions due to the Poisson ratio; as a result, the dissipation is reduced compared to the uniaxial strain case because $\alpha_{\text{WE}}^2 < 1$. In the SE mode, the solid expands in x and y (and contracts in z) so that the deformation of the mechanical mode resists the natural contraction of the solid. The perturbations of x and y add constructively, leading to increased dissipation compared to the WE mode. This leads to reduced Q despite the fact that the SE mode has a higher energy storage density than the WE mode. In the CE mode, the solid expands in the x , y , and z directions resulting in the largest combined perturbation and energy dissipation and the smallest Q . Our results indicate that the quality factor limits for silicon at a specified resonant frequency can vary by more than an order of magnitude when including anisotropic energy storage and loss ($Q_{\text{WE}} \approx 2.5 Q_{\text{SE}} \approx 23.5 Q_{\text{CE}}$).

The Lamé mode has the highest upper bound on Q for the modes considered in this work, despite having the smallest energy storage modulus. This is an important consequence of the condition that shear vibration modes preserve volume. In a pure-shear vibration, the mode-Grüneisen parameters for longitudinal phonon branches do not contribute, because these perturbations would change the volume of the solid. Effectively, the phonon-phonon scattering for shear vibrations is limited to the

volume-preserving transverse phonon branches, which leads to reduced energy dissipation because fewer branches, and less phonon energy, are subject to the relaxation process. This result indicates that Lamé mode resonators may be the best candidates for ultrahigh Q silicon resonators. We note that Woodruff's isotropic formula actually predicts infinite Q (zero dissipation) for shear modes because the average Grüneisen parameter [γ_0 in Eq. (1)] for volume-preserving modes is zero. The limitations of Woodruff's expression have been acknowledged in the past [12,16], but we provide a viable alternative expression that shows that shear-mode vibrations do in fact lead to anharmonic phonon-phonon dissipation.

The evaluation of the anharmonic and anisotropic expression derived in this work indicates that Woodruff's order-of-magnitude result (dashed line) fails to provide an upper bound on the quality factor due to Akhiezer damping. In fact, several silicon resonators with quality factors that exceed Woodruff's limit have already been fabricated and measured in the literature [26–29], indicating the important need for our more accurate damping model that provides a robust upper bound on the performance of modern micro-mechanical resonators.

The experimental points are broadly categorized by geometry and mode type. The highest Q resonators of a given type are grouped horizontally, reinforcing the assertion that the $f \times Q$ product is constant for a particular mode shape, in accordance with Eq. (24). It is important to convey the fact that the evaluation of Eq. (24) provides an upper bound on the quality factor, so it only predicts the performance of devices that are limited by anharmonic phonon-phonon dissipation, meaning other loss mechanisms including TED, air-damping, and anchor loss have insignificant contributions. We also note that the theory lines in Fig. 3 use the idealized mode profiles in Table I, and, consequently, do not necessarily predict the exact behavior of the devices included as experimental references, because the actual vibrational modes are complicated functions of the geometry and boundary conditions of the structure. Additionally, the results here are for intrinsic silicon, and do not account for variations due to dopant species and density. The most accurate results can be obtained if the doping dependencies of second- and third-order elastic coefficients and thermal conductivity, which determines τ , are known [44].

VII. CONCLUSION

In this work, we provide an analytical expression for the quality factor due to anharmonic phonon-phonon dissipation that explicitly includes the anisotropic energy storage and loss in a cubic semiconductor or dielectric crystal. We provide a rigorous derivation of the anharmonic loss using the phonon BTE and introduce the important simplifications that must be made in order to facilitate quality factor

calculation using known material parameters. These simplifications are presented and justified in Secs. III–V and evaluated for the most common vibration modes for [100] silicon in Sec. VI. Our advanced model combined with relatively straightforward evaluation allows for meaningful comparisons between theory and experimental results and provides insight into the efficiency of different vibrational modes in the Akhiezer dissipation limit. Despite having lower energy storage moduli, the Lamé and width-extensional vibration modes have the highest potential quality factor, meaning they are the best candidates for high-performance, Akhiezer-limited resonators. The formulations introduced in this work can easily be extended to account for doping dependence (when appropriate material data are available) and integrated into a finite-element solver to provide the most accurate predictions of phonon-phonon dissipation for *arbitrary* vibration profiles, including higher-order modes, in cubic crystals.

ACKNOWLEDGMENTS

This work was supported by the Army Research Office under Contract No. W911NF-12-1-0190 and the Defense Advanced Research Projects Agency and U.S. Navy under Contract No. N66001-13-1-4032.

-
- [1] V. B. Braginsky, V. P. Mitrofanov, V. I. Panov, and C. Eller, *Systems with Small Dissipation* (University of Chicago Press, Chicago, 1985).
 - [2] P. S. Waggoner and H. G. Craighead, Micro- and nano-mechanical sensors for environmental, chemical, and biological detection, *Lab Chip* **7**, 1238 (2007).
 - [3] P. Mohanty, D. A. Harrington, K. L. Ekinci, Y. T. Yang, M. J. Murphy, and M. L. Roukes, Intrinsic dissipation in high-frequency micromechanical resonators, *Phys. Rev. B* **66**, 085416 (2002).
 - [4] R. N. Candler, A. Duwel, M. Varghese, S. A. Chandorkar, M. Hopcroft, W.-T. Park, B. Kim, G. Yama, A. Partridge, M. Lutz, and T. W. Kenny, Impact of geometry on thermoelastic dissipation in micromechanical resonant beams, *J. Microelectromech. Syst.* **15**, 927 (2006).
 - [5] S. A. Chandorkar, R. N. Candler, A. Duwel, R. Melamud, M. Agarwal, K. E. Goodson, and T. W. Kenny, Multimode thermoelastic dissipation, *J. Appl. Phys.* **105**, 043505 (2009).
 - [6] W. P. Mason, *Physical Acoustics: Principles and Methods*, edited by W. P. Mason (Academic Press Inc., New York, 1965), Vol. IIIB.
 - [7] A. Akhiezer, On the absorption of sound in solids, *J. Phys. USSR* **1**, 277 (1939).
 - [8] T. O. Woodruff and H. Ehrenreich, Absorption of sound in insulators, *Phys. Rev.* **123**, 1553 (1961).
 - [9] S. Ghaffari, S. A. Chandorkar, S. Wang, E. J. Ng, C. H. Ahn, V. Hong, Y. Yang, and T. W. Kenny, Quantum limit of quality factor in silicon micro and nano mechanical resonators, *Nat. Sci. Rep.* **3**, 3244 (2013).

- [10] W. P. Mason and T. B. Bateman, Ultrasonic-wave propagation in pure silicon and germanium, *J. Acoust. Soc. Am.* **36**, 644 (1964).
- [11] A. N. Cleland, *Foundations of Nanomechanics: From Solid-State Theory to Device Applications* (Springer Science & Business Media, Berlin, 2013).
- [12] H. H. Barrett and M. G. Holland, Critique of current theories of Akhiezer damping in solids, *Phys. Rev. B* **1**, 2538 (1970).
- [13] G. G. Sahasrabudhe and S. D. Lambade, Temperature dependence of the collective phonon relaxation time and acoustic damping in Ge and Si, *J. Phys. Chem. Solids* **60**, 773 (1999).
- [14] L. G. Merkulov, R. V. Kovalenok, and E. V. Konovodehenko, Orientation dependence of the absorption of ultrasound in alkali halide crystals, *Fiz. Tverd. Tela* **11**, 2241 (1970).
- [15] S. D. Lambade, G. G. Sahasrabudhe, and S. Rajagopalan, Temperature dependence of acoustic attenuation in silicon, *Phys. Rev. B* **51**, 15861 (1995).
- [16] A. Nowick and D. Berry, *Anelastic Relaxation in Crystalline Solids* (Academic Press, New York, 1972).
- [17] R. Nava, M. P. Vecchi, J. Romero, and B. Fernandez, Akhiezer damping and the thermal conductivity of pure and impure dielectrics, *Phys. Rev. B* **14**, 800 (1976).
- [18] A. A. Kiselev and G. J. Iafrate, Phonon dynamics and phonon assisted losses in Euler-Bernoulli nanobeams, *Phys. Rev. B* **77**, 205436 (2008).
- [19] H. E. Bömmel and K. Dransfeld, Excitation and attenuation of hypersonic waves in quartz, *Phys. Rev.* **117**, 1245 (1960).
- [20] K. Kunal and N. R. Aluru, Akhiezer damping in nanostructures, *Phys. Rev. B* **84**, 245450 (2011).
- [21] M. Hopcroft, W. D. Nix, and T. W. Kenny, What is the Young's modulus of silicon?, *J. Microelectromech. Syst.* **19**, 229 (2010).
- [22] V. P. Mitrofanov, L. G. Ovodova, and V. S. Shiyan, Longitudinal sound-wave attenuation in sapphire due to phonon-phonon interaction, *Fiz. Tverd. Tela (Leningrad)* **22**, 1545 (1980).
- [23] C. Kittel, *Introduction to Solid State Physics* (Wiley, New York, 2005).
- [24] Y. V. Ilisavskii and V. M. Sternin, Lattice absorption of high-frequency sound in silicon, *Fiz. Tverd. Tela* **27**, 236 (1985).
- [25] R. Tabrizian, M. Rais-Zadeh, and F. Ayazi, Effect of phonon interactions on limiting the $f \cdot Q$ product of micromechanical resonators, in *Proceedings of the IEEE International Conference on Solid State Sensors, Actuators and Microsystems, Denver, 2009* (IEEE, New York, 2009), pp. 2131–2134.
- [26] G. Wu, D. Xu, B. Xiong, and Y. Wang, High Q single crystal silicon micromechanical resonators with hybrid etching process, *IEEE Sens. J.* **12**, 2414 (2012).
- [27] D. Weinstein and S. Bhave, Internal dielectric transduction in bulk-mode resonators, *J. Microelectromech. Syst.* **18**, 1401 (2009).
- [28] S.-S. Li, Y.-W. Lin, Y. Xie, Z. Ren, and C. T.-C. Nguyen, Micromechanical “hollow-disk” ring resonators, in *Proceedings of the 17th IEEE International Conference on Micro Electro Mechanical Systems (MEMS), 2004* (IEEE, New York, 2004), pp. 821–824.
- [29] M. Ziaei-Moayyed and R. T. Howe, Higher-order dielectrically transduced bulk-mode ring resonator with low motional resistance, in *Proceedings of the IEEE International Frequency Control Symposium (FCS), Newport Beach, 2010* (IEEE, New York, 2010), pp. 19–24.
- [30] L. Khine and M. Palaniapan, High- Q bulk-mode SOI square resonators with straight-beam anchors, *J. Micromech. Microeng.* **19**, 015017 (2009).
- [31] J. E.-Y. Lee and A. A. Seshia, 5.4-MHz single-crystal silicon wine glass mode disk resonator with quality factor of 2 million, *Sens. Actuators A* **156**, 28 (2009).
- [32] S. Pourkamali, G. K. Ho, and F. Ayazi, Low-impedance VHF and UHF capacitive silicon bulk acoustic-wave resonators—Part II: Measurement and characterization, *IEEE Trans. Electron Devices* **54**, 2024 (2007).
- [33] A. K. Samaroo, G. Casinovi, and F. Ayazi, Passive TCF compensation in high Q silicon micromechanical resonators, in *Proceedings of the 23rd IEEE International Conference on Micro Electro Mechanical Systems (MEMS), 2010* (IEEE, New York, 2010), pp. 116–119.
- [34] H. M. Lavasani, A. K. Samaroo, G. Casinovi, and F. Ayazi, A 145 MHz low phase-noise capacitive silicon micromechanical oscillator, in *Proceedings of the International Electron Devices Meeting, San Francisco, 2008* (IEEE, New York, 2008), pp. 1–4.
- [35] J. E.-Y. Lee, B. Bahreyni, Y. Zhu, and A. Seshia, A single-crystal-silicon bulk-acoustic-mode microresonator oscillator, *IEEE Electron Device Lett.* **29**, 701 (2008).
- [36] C. Tu and J. E.-Y. Lee, Increased dissipation from distributed etch holes in a lateral breathing mode silicon micromechanical resonator, *Appl. Phys. Lett.* **101**, 023504 (2012).
- [37] H. Zhu, Y. Xu, and J. E.-Y. Lee, Piezoresistive readout mechanically coupled Lamé mode SOI resonator with Q of a million, *J. Microelectromech. Syst.* **24**, 771 (2015).
- [38] J. Wang, Z. Ren, and C. T.-C. Nguyen, 1.156-GHz self-aligned vibrating micromechanical disk resonator, *IEEE Trans. Ultrason. Ferroelectr. Freq. Control* **51**, 1607 (2004).
- [39] J. R. Clark, W.-T. Hsu, M. Abdelmoneum, and C. T.-C. Nguyen, High- Q UHF micromechanical radial-contour mode disk resonators, *J. Microelectromech. Syst.* **14**, 1298 (2005).
- [40] L. Landau and G. Rumer, Absorption of sound in solids, *Phys. Z. Sowjetunion* **11** (1937).
- [41] Y. S. Ju and K. E. Goodson, Phonon scattering in silicon films with thickness of order 100 nm, *Appl. Phys. Lett.* **74**, 3005 (1999).
- [42] F. Yang and C. Dames, Mean free path spectra as a tool to understand thermal conductivity in bulk and nanostructures, *Phys. Rev. B* **87**, 035437 (2013).
- [43] K. T. Regner, D. P. Sellan, Z. Su, C. H. Amon, A. J. H. McGaughey, and J. A. Malen, Broadband phonon mean free path contributions to thermal conductivity measured using frequency domain thermoreflectance, *Nat. Commun.* **4**, 1640 (2013).
- [44] E. J. Ng, V. A. Hong, Yushi Yang, Chae Hyuck Ahn, C. L. M. Everhart, and T. W. Kenny, Temperature dependence of the elastic constants of doped silicon, *J. Microelectromech. Syst.* **24**, 730 (2015).